CHEMICAL ENGINEERING TRANSACTIONS
VOL. 109, 2024
A publication of AIDIC
The Italian Association of Chemical Engineering
Online at www.cetjournal.it
Guest Editors: Leonardo Tognotti, Rubens Maciel Filho, Viatcheslav Kafarov

ISBN 979-12-81206-09-0; **ISSN** 2283-9216
DOI: 10.3303/CET24109109

Analysis of Natural Convection During the Melting Process of Hydrogenated Palm Stearin for use as Phase-Change Material

Víctor A. Lizcano-González[a], Viatcheslav Kafarov[a] , Khamid Mahkamov[b], Valentina Aguilera-Duarte[a], Anamaria Blanco-Beltran[a]

[a]Department of Chemical Engineering, Carrera 27 Calle 9, Universidad Industrial de Santander, Bucaramanga, Colombia
[b]Department of Mechanical and Construction Engineering, Sutherland Building Newcastle-upon-Tyne NE1 8ST, Northumbria University, United Kingdom
kafarov@uis.edu.co

There are three main alternatives for the improvement of heat transfer in phase change materials (PCM) such as the use of additives, support matrices and customized designs for heat exchangers. The first two alternatives imply incurring additional material costs, as well as a decrease in the specific heat storage capacity by using components that remain solid during the process. The present work therefore sought to study the effect of the use of a coil shell heat exchanger with a square cross section on natural convection during the melting process of hydrogenated palm stearin. Three different sections of the profile called square profile, U-profile, and L-profile and two types of material, copper, and stainless steel, were studied. A test bench was built with a capacity of 5 kg of this PCM, implementing a hot water recirculation system with flow and temperature measurement and including 9 temperature sensors inside the PCM. The melting process was conducted by recirculating water with a temperature of 75° C and a flow rate of 2 L/min. The results show a marked effect of natural convection on the melting process, presenting characteristic profiles for this phenomenon. It was found that the highest temperatures are recorded in the upper part of the PCM and that the heat transfer in the solid material is appreciably low. The results allow us to identify for each profile, the zones in which heat transfer is relatively high because of natural convection and those zones that require the use of additives or support matrices. It is therefore expected to contribute to the design of more efficient and lower commercial cost configurations.

1. Introduction

Solar energy can be harnessed to produce electricity or heat (Mohammad et al., 2022), however, natural factors such as rain, wind, and day length, generate the need to implement storage systems (Mofijur et al., 2019). An alternative for solar thermal energy storage is the use of contained phase change materials (PCMs) in heat exchangers (Youssef et al., 2018). PCMs are materials that transform from solid to liquid state when they store heat and then reverse when they release energy (Shen et al., 2022). For latent heat storage, PCMs must have certain characteristics such as an appropriate melting temperature for the application, chemical stability, and high thermal conductivity (Liu et al., 2021). Some of these characteristics are found in naturally derived organic materials such as beeswax, palm stearin, or hydrogenated palm stearin. The latter stands out for its melting temperature of 59 °C, suitable for heating or hot water supply applications (Lizcano-González et al., 2023). The design of these heat exchangers should seek to maximize the energy transfer rate so alternatives such as support matrices, additives and modifications in the geometrical configuration are used (Momeni et al., 2023). Regarding the latent heat storage system, different geometric configurations for PCM housings have been proposed: spherical housings, tall rectangular housings, and cylindrical tubes (Sciacovelli et al., 2013). The most studied geometric variants are the tube-shell heat exchanger with or without fins. Improvements in the lauric acid fusion time have been reported for its use as PCM using a tube-shell heat exchanger system with four different arrangements. In heat exchangers, the most common heat transfer mechanism is natural convection, characterized by fluid movement due to buoyancy differences induced by temperature variations (Amoo, 2020).

Paper Received: 30 November 2023; Revised: 7 February 2024; Accepted: 5 April 2024
Please cite this article as: Lizcano-González V.A., Kafarov V., Mahkamov K., Aguilera-Duarte V., Blanco-Beltran A., 2024, Analysis of Natural Convection During the Melting Process of Hydrogenated Palm Stearin for Use as Phase-change Material, Chemical Engineering Transactions, 109, 649-654 DOI:10.3303/CET24109109

Natural convection played an important role in the lauric acid fusion, accelerating the process and reducing the fusion time by approximately 70% in configurations where the tubes were located at the bottom of the housing (Mahdi et al., 2021). The performance of palmitic acid as PCM has also been studied in a system of circular tubes arranged vertically and horizontally. It was concluded that the fusion time was significantly reduced when the tube containing the PCM was in a horizontal position. This improvement was since in this orientation, the fusion front had to cover a shorter distance radially at the top of the tube, facilitating natural convection (Hasan, 1994). Only a few studies report the use of the shell-coil configuration. The coil-shell configuration has an advantage in terms of construction costs due to its simplicity, lower number of components and shorter assembly time. One of these conducted an experimental study on a PCM cold storage system with a tank coil. The study demonstrated that using coils in storage unit designs is effective for transferring heat over large surfaces (Castell et al., 2011). An experimental investigation of the performance of an energy storage system with xylitol as PCM in a heat exchanger with a spiral coil was reported. The PCM stored 450 kJ of heat in 35 minutes during charging and 345 kJ in 50 minutes for the discharging process. It was found that as the PCM melted, the lower density liquid PCM created buoyancy forces resulting in natural convection. On the other hand, the discharge process was primarily governed by conduction (Anish et al., 2021). Therefore, the main objective of this work is to experimentally evaluate the melting process of hydrogenated palm stearin for its potential use as PCM in coil shell systems. It is necessary to understand how the coil design and its construction material influence the melting process of hydrogenated palm stearin using a U and square shaped coil. This is in order to quantify the effect of natural convection on this recently reported new PCM, which will facilitate the future design of heat exchangers.

2. Materials and Methods

The experimental study system consists of a test bench made of acrylic material (see Figure 1), specifically designed to evaluate PCM melting processes. The test rig was equipped with a total of nine DS18B20-type sensors, positioned to measure the temperature of the PCM. The spatial arrangement of these sensors within the test bench is described in Figure 1. A Hall effect flow meter and two extra temperature sensors were used for measurement conditions of heat transfer fluid (HTF). To maintain a constant temperature of the HTF between 74-75 °C with a flow rate of 2.5 ± 0.5 L min^{-1}, a thermal bath with a water recirculation system was employed.

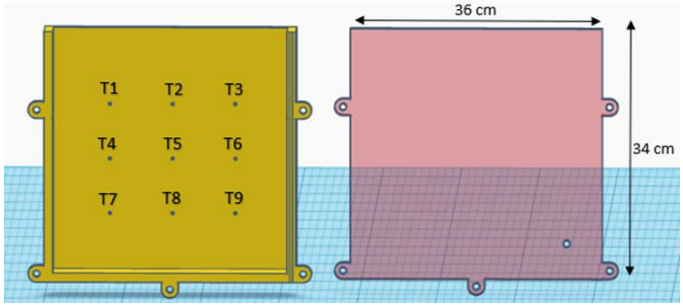

Figure 1:Test bench and sensor locations.

The experimental tests consisted of subjecting hydrogenated palm stearin to melting processes, using copper coils with two different geometric configurations: one square-shaped and the other U-shaped (see Figure 2).

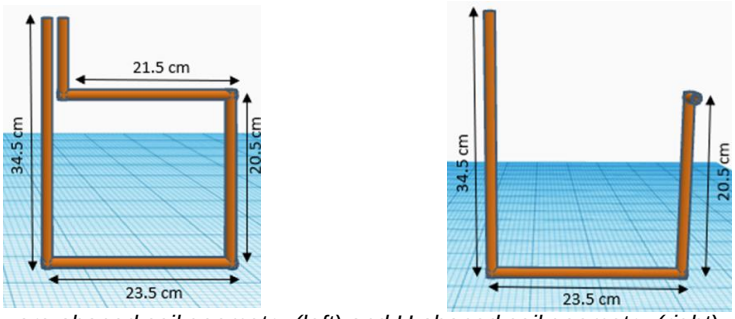

Figure 2: Square-shaped coil geometry (left) and U-shaped coil geometry (right).

The system was insulated using 1.5 cm thick expanded polystyrene. Additionally, the setup was installed inside a closed chamber to prevent the presence of air currents. Subsequently, data processing was conducted using an algorithm programmed in MATLAB (MathWorks, Inc.).

The heat transferred from the heat transfer fluid to the PCM was calculated using the formula:

$$\boldsymbol{Q = \dot{m} \cdot C_{pT} \cdot \Delta T} \quad (1)$$

$\dot{m}$ represents the mass flow, C_{pT} the heat capacity and ΔT the temperature difference between the fluid inlet and outlet. The convective heat transfer coefficient h was calculated as follows (Pakalka et al., 2021):

$$\boldsymbol{h = \frac{Q}{A_{PCM} \cdot (T_{HX} - T_{PCM})}} \quad (2)$$

Where Q denotes the heat transferred during the process, A_{PCM} corresponds to heat transfer area, is T_{PCM} the sensor temperature, T_{HX} represents the average of the fluid inlet and outlet temperatures. The evaluation of this coefficient provided essential information on how the geometry of the system affects heat transfer, thus providing key insight into the specific characteristics of the experimental process studied.

3. Results and Discussion

Table 1: Time in which the first heat transfer coefficients appear for the square and U-shaped coil casing geometries, as well as for the tube and fin configuration found in the literature.

Geometry	h (W m^{-2} K^{-1})	Time (min)	References
Square coil casing	578	120	Authors
Coil casing U	533	120	Authors
Fin and tube	50	8	Pakalka et al., 2021

In Table 1 we observe the time at which the first heat transfer coefficients (h) appear for the two configurations studied and for a tube and fin geometry found in the literature. The heat transfer coefficient is applicable to any geometry, depending on the physical properties of the PCM, the configuration of the heat transfer surface and the surrounding flow conditions. In the fin and tube geometry, the first heat transfer coefficients (h) appeared after 8 minutes of the test, averaging 50 (W m^{-2} K^{-1}). In the square coil shell geometry, the first heat transfer coefficients (h) were observed after 120 minutes, with an average value of 578 (W m^{-2} K^{-1}). Finally, in the U-shaped coil casing geometry, the heat transfer coefficients (h) showed an average of 533 (W m^{-2} K^{-1}), after 120 min. Figure 3 shows the time and temperature values recorded during the 24 hours of testing at the nine measurement points for the square copper geometry. The convective heat transfer coefficients (h) were calculated once the sensor recorded a temperature higher than 48.5 °C (TF), the temperature at which the PCM melts. According to the data recorded, the times to reach the melting temperature (TF) in the sensors were: T7 and T9, 2 hours; T8, three hours; T1 and T4, 4 hours; T3, 5 hours; T6, 6 hours; T2, 9 hours; T5, 13 hours. It should be noted that the sensor that took the longest time to reach TF is the one located right in the middle of the test bench, being far away from all the pipe sections. The fast response of the T7 and T9 sensors can be attributed to the location near the lower corners of the coil. It is inferred that by being located close to two sections of the coil and having an upward heat flow, heat transfer is higher compared to other sensors. There was heating from the bottom of the PCM maximizing natural convection and consequently heat transfer (Hasan, 1994). In the case of T8, heating from the bottom of the sensor is also present. Regarding the h values, these were analyzed by time intervals, corresponding to hour 0 to 12 and from hour 12 to 24. It was evidenced that h7, h8 and h9 presented an accelerated growth after the first 2 hours due to the horizontally oriented pipe section that was located just below the sensors and promoted the melting of the material. The rapid increase ceased at hour 8 as temperatures stabilized. From hour 12 to 24 they maintained values above 1000 W m^{-2} K^{-1} with small fluctuations. This behavior is explained by the location of the sensors close to a pipe section placed below it. In contrast, h1 and h3 in the first-time interval presented a slow growth due to low convection because of the location of the heat transfer fluid inlet. However, both coefficients experienced an increase during the second time interval. It should be noted that, at the end of the second time interval, the highest values of h were calculated with respect to all the measurement points. These high values of h are mainly explained by the less dense PCM that creates buoyancy forces that generate an upward movement favoring the natural convection that affects the upper part of the test bench unit (Seddegh et al., 2016). Regarding h2, in the first part of the test it grows slowly compared to the surrounding sensors. However, in the second time section it presents the highest h values of the whole test, this is explained by it was in the middle of two zones that presented a large amount of molten material.

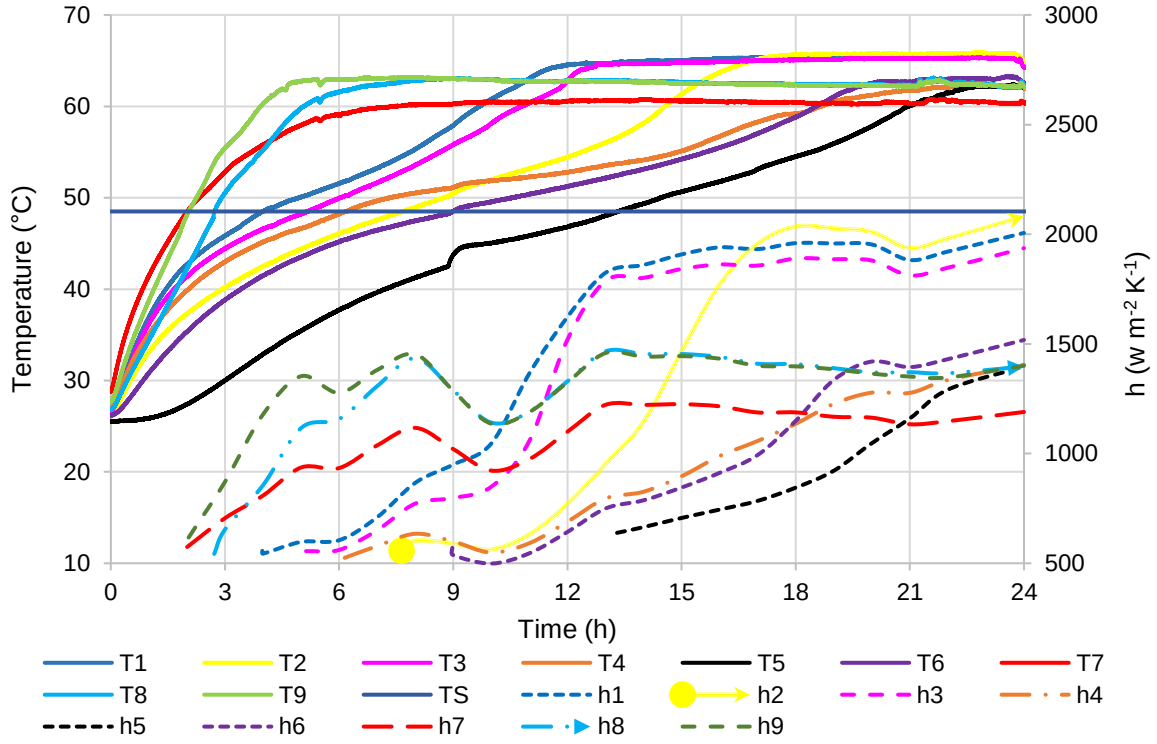

Figure 3:Temperature variation and local heat transfer coefficient at different measurement points for the square coil geometry are presented. The evolution of temperature in the nine sensors, along with the corresponding values of the coefficient h, is shown once the sensor reaches a temperature of 48.5°C.

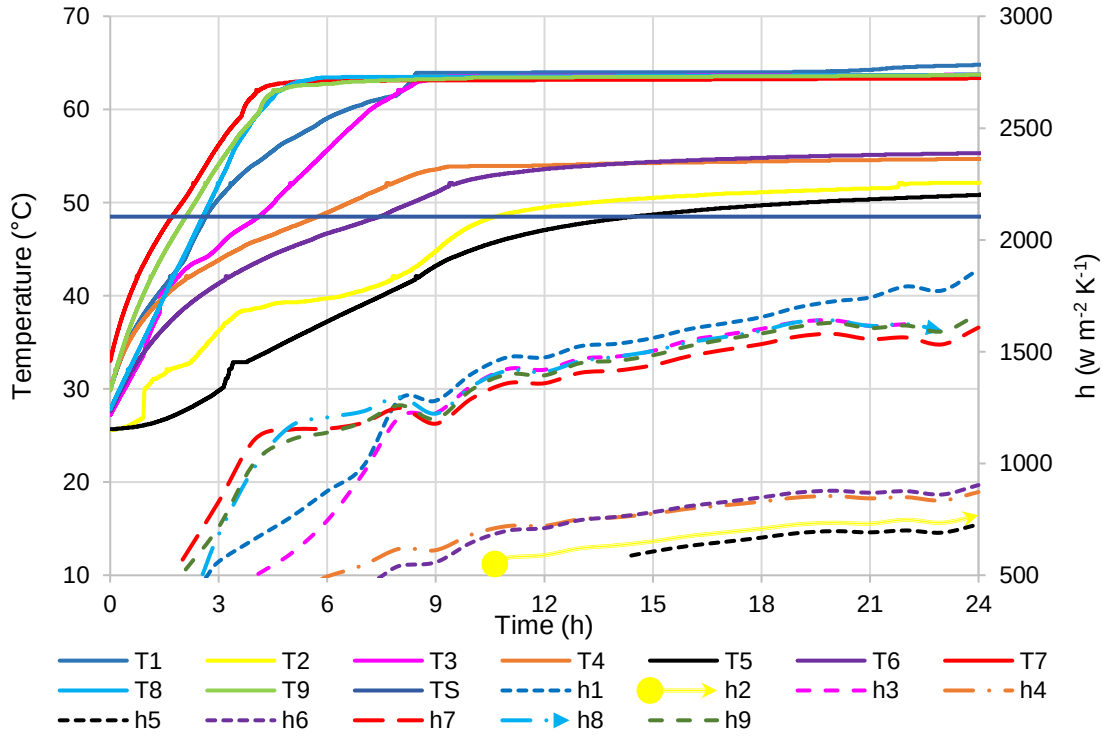

Figure 4:Temperature variation and local heat transfer coefficient at different measurement points for the U coil geometry are presented. The evolution of temperature in the nine sensors, along with the corresponding values of the coefficient 'h,' is shown once the sensor reaches a temperature of 48.5 °C.

During the first 12 hours of testing, h4 and h6 grew slowly. But, in the second period they presented values greater than 500 W m-2 K-1. The h5 coefficient presented values only in the second time interval, which were the lowest in comparison to all the calculated h values. It is relevant to note that, for this section (h4, h5, h6) the location did not favor convection due to the orientation of the nearby pipe, as previously mentioned. Consequently, the PCM remained in solid state for a large amount of time and in that state of aggregation it did not conduct heat adequately. Heating from the bottom of the PCM maximized natural convection, which resulted in higher heat transfer (Mahdi et al., 2019). Likewise, in the case of T8, heating from the bottom of the sensor was also observed. In general terms, it is concluded that heat transfer occurs at a higher rate in the upward vertical direction (See **Figure 5**). **Figure 4** presents the time and temperature values recorded during the 24-hour test period at the nine measurement points for the copper U-shaped geometry. The convective heat transfer coefficients (h) were calculated when the sensor registered a temperature above 48.5 °C, the melting temperature of the PCM. Regarding the h values (convective heat transfer coefficients), they were analyzed at two-time intervals: from hour 0 to 12 and from hour 12 to 24. It was revealed that h7, h8 and h9 showed an accelerated growth after the first 2 hours due to the horizontally oriented tube section located just below the sensors, which favored the melting of the material. The increase in h values stabilized around hour 4, when the temperatures reached equilibrium. From hour 12 to 24, h values remained above 1000 W m-2 K-1 with slight fluctuations. This behavior is explained by the specific location of the sensors, as previously reported by other authors (Anish et al., 2021). On the other hand, h1 and h3 showed slow growth during the first-time interval. Like the h coefficients mentioned in the previous paragraph, there was a slight decrease in their values that coincided with the stabilization of temperatures. However, both coefficients increased remarkably during the second time interval. It is important to highlight that, at the end of the second time interval, the highest values of h were calculated compared to all other measurement points (Mahdi et al., 2019). As for h2, it showed slower growth during the initial phase of the test compared to the surrounding sensors. Moreover, in the second time interval, it showed the lowest h values among all measurement points throughout the entire test. This can be explained by the fact that h2 had no nearby pipe and, despite being located between two zones with significant melting activity, it was not sufficient for the PCM to melt at that point.

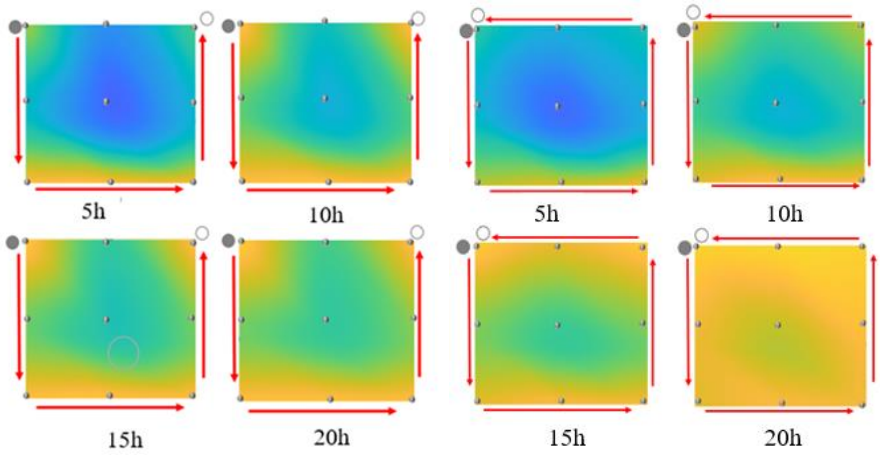

Figure 5:Temperature distribution in the melting process for U (left) and square (right) geometry at t=5h, t=10h, t=15h, and t=20h.

4. Conclusions

In conclusion, the two configurations were able to achieve PCM melting within 24 hours of the experiment. However, they presented significant differences in terms of heat transfer and homogeneity of the process. The square geometry showed a more complete and uniform melting, with all sensors reaching the melting temperature (TF) of 60 °C at the end of the test. This suggests a more uniform distribution throughout the PCM volume. In contrast, the U-shaped geometry exhibited less uniform melting, with only five sensors reaching temperatures above 60 °C. Four sensors (T2, T4, T5, T6) failed to reach the PCM melting temperature, indicating that heat transfer was less homogeneous at certain locations in the system. This behavior shows the positive effect that the rapid melting of the upper layer of the PCM has on the heat transfer rate, because it creates a free movement zone for the liquid PCM, which allows high values of natural convection.

Although the complete fusion of the PCM with the U-shaped geometry was not achieved, this configuration showed high heat transfer coefficients (h), which added to a 25% saving of the material used, could be used as a basis for the development of minimum cost heat exchangers.

Acknowledgments

Special thanks to the Vice-Rectory of Research and Extension of the Universidad Industrial de Santander for their support to the project " Estudio de la Convección Natural Durante La Fusión de Materiales de Cambio de Fase para el Almacenamiento de Energía Solar Térmica En Sistemas Carcasa-Serpentín", code VIE 3732. Authors also would like to thank The Royal Society for supporting the research entitled Enabling Harvesting of Solar Energy for Remote Applications in the Andes Region (LA-SOLAR ENHANCE- ICA\R1\191201). Also special thanks to the Ministerio de Ciencia Tecnología e Innovación of Colombia for the support of the project entitled “Desarrollo de una herramienta metodológica computacional y tecnologías de energías renovables para la transición energética en zonas de alta montaña en condiciones de post- pandemia”, CD 82605 CT ICETEX 2022-0644.

References

Amoo L.M., 2020, On a selection of the applications of thermodynamics, Chapter In: R.O. Fagbenle, O.M. Amoo, S. Aliu, A. Falana (Ed.), Applications of Heat, Mass and Fluid Boundary Layers, Woodhead Publishing Limited, Cambridge, UK.

Anish R., Mariappan V., Suresh S., Joybari M.M., Abdulateef A.M, 2021, Experimental investigation on the energy storage/discharge performance of xylitol in a compact spiral coil heat exchanger, International Journal of Thermal Sciences, 159, 106633.

Castell A., Belusko M., Bruno F., Cabeza L.F., 2011, Maximisation of heat transfer in a coil in tank PCM cold storage system, Applied Energy, 88, 4120-4127.

Hasan A., 1994, Phase change material energy storage system employing palmitic acid, Solar Energy, 52, 143-154.

Liu Y., Zheng J., Deng Y., Wu F., Wang H., 2021, Effect of functional modification of porous medium on phase change behavior and heat storage characteristics of form-stable composite phase change materials: A critical review, Journal of Energy Storage, 44, 103637.

Lizcano-González V.A., Kafarov V., Mahkamov K., Arciniegas C., Socha Rojas, M.P., 2023, Potential Application of Renewable Eutectic Mixtures as Phase Change Materials for Thermal Energy Storage, Chemical Engineering Transactions, 99, 391-396.

Mahdi M.S., Hasan A.F., Mahood H.B., Campbell A.N., Khadom A.A., Karim A.M., Em A., Sharif A.O., 2019, Numerical study and experimental validation of the effects of orientation and configuration on melting in a latent heat thermal storage unit, Journal of Energy Storage, 23, 456-468.

Mahdi M.S., Mahood H.B., Khadom A.A., Campbell A.N., 2021, Numerical simulations and experimental verification of the thermal performance of phase change materials in a tube-bundle latent heat thermal energy storage system, Applied Thermal Engineering, 194, 117079.

Mofijur M., Mahlia T.M.I., Silitonga A.S., Ong H.C., Silakhori M., Hasan M.H., Putra N., Ashrafur Rahman S.M., 2019, Phase change materials (PCM) for solar energy usages and storage: An overview, Energies, 12, 3167.

Mohammad S.S., Iqbal S.J., Lone R.A., 2022, Improved Utilization of Solar Energy Using Estimated Optimal Tilt Factor and Trackers, Energy Reports, 8, 175–183.

Momeni M., Fartaj A., 2023, Numerical thermal performance analysis of a PCM-to-air and liquid heat exchanger implementing latent heat thermal energy storage, Journal of Energy Storage, 58, 106363.

Pakalka S., Valančius K., Streckienė G., 2021, Experimental and theoretical investigation of the natural convection heat transfer coefficient in phase change material (PCM) based fin-and-tube heat exchanger, Energies, 14, 716.

Sciacovelli A., Colella F., Verda V., 2013, Melting of PCM in a thermal energy storage unit: Numerical investigation and effect of nanoparticle enhancement, International Journal of Energy Research, 37, 1610–1623.

Seddegh S., Wang X., Henderson A.D., 2016, A comparative study of thermal behaviour of a horizontal and vertical shell-and-tube energy storage using phase change materials, Applied Thermal Engineering, 93, 348–358.

Shen R., Liu L., Cao Y., Zhang L., Sheng X., Chen Y., 2022, Biomass modified boron nitride/polyimide hybrid aerogel supported phase change composites with superior energy storage capacity and improved flame retardancy for solar-thermal energy storage, Solar Energy, 242, 287–297.

Youssef W., Ge Y.T., Tassou S.A., 2018, CFD modelling development and experimental validation of a phase change material (PCM) heat exchanger with spiral-wired tubes, Energy Conversion and Management, 157, 498-510.